JOURNAL OF GEOPHYSICAL RESEARCH, VOL. 112, D04102, doi:10.1029/2006JD007222, 2007

Click Here for Full Article

Electromagnetic models of the lightning return stroke

Yoshihiro Baba[1] and Vladimir A. Rakov[2]

Received 24 February 2006; revised 22 August 2006; accepted 6 October 2006; published 16 February 2007.

[1] Lightning return-stroke models are needed for specifying the source in studying the production of transient optical emission (elves) in the lower ionosphere, the energetic radiation from lightning, and characterization of the Earth's electromagnetic environment, as well as studying lightning interaction with various objects and systems. Reviewed here are models based on Maxwell's equations and referred to as electromagnetic models. These models are relatively new and most rigorous of all models suitable for computing lightning electromagnetic fields. Maxwell's equations are numerically solved to yield the distribution of current along the lightning channel. Different numerical techniques, including the method of moments (MoM) and the finite difference time domain (FDTD) method, are employed. In order to achieve a desirable current-wave propagation speed (lower than the speed of light in air), the channel-representing wire is embedded in a dielectric (other than air) or loaded by additional distributed series inductance. Capacitive loading has been also suggested. The artificial dielectric medium is used only for finding the distribution of current along the lightning channel, after which the channel is allowed to radiate in air. Resistive loading is used to control current attenuation with height. In contrast with distributed circuit and so-called engineering models, electromagnetic return-stroke models allow a self-consistent full-wave solution for both lightning-current distribution and resultant electromagnetic fields. In this review, we discuss advantages and disadvantages of four return-stroke channel representations: a perfectly conducting/resistive wire in air, a wire embedded in a dielectric (other than air), a wire in air loaded by additional distributed series inductance, and a wire in air having additional distributed shunt capacitance. Further, we describe and compare different methods of excitation used in electromagnetic return-stroke models: closing a charged vertical wire at its bottom with a specified grounded circuit, a delta-gap electric field source, and a lumped current source. Finally, we review and compare representative numerical techniques used in electromagnetic modeling of the lightning return stroke: MoMs in the time and frequency domains and the FDTD method. We additionally consider the so-called hybrid model of the lightning return stroke that employs a combination of electromagnetic and circuit theories and compare this model to electromagnetic models.

Citation: Baba, Y., and V. A. Rakov (2007), Electromagnetic models of the lightning return stroke, *J. Geophys. Res.*, *112*, D04102, doi:10.1029/2006JD007222.

1. Introduction

[2] Lightning return-stroke models are needed in a variety of geophysical studies, including the production of transient optical emission (elves) in the lower ionosphere [e.g., *Krider*, 1994; *Rakov and Tuni*, 2003; *Lu*, 2006], the energetic radiation from lightning [e.g., *Inan and Lehtinen*, 2005], and characterization of the lightning electromagnetic environment [e.g., *Kordi et al.*, 2003b], as well as in studying lightning effects on various objects and systems [e.g., *Moini et al.*, 1998]. Clearly, conclusions drawn from these studies are influenced by the choice and validity of lightning source model employed [e.g., *Thottappillil et al.*, 1997; *Rakov and Tuni*, 2003]. *Rakov and Uman* [1998], based on governing equations, have categorized return-stroke models into four classes: gas dynamic models, electromagnetic models, distributed circuit models, and ''engineering'' models. Out of these four classes, electromagnetic models and engineering models are most widely used in lightning electromagnetic field calculations.

[3] Engineering return-stroke models are equations relating the longitudinal current along the lightning channel at any height and any time to the current at the channel origin (the origin is usually situated at ground level, but can be at the top of a tall grounded strike object [e.g., *Rachidi et al.*,

[1]Department of Electrical Engineering, Doshisha University, Kyoto, Japan.
[2]Department of Electrical and Computer Engineering, University of Florida, Gainesville, Florida, USA.

Copyright 2007 by the American Geophysical Union.
0148-0227/07/2006JD007222$09.00

2002]). The return-stroke wavefront speed in these models can be set arbitrarily, since it is one of the input parameters. Engineering return-stroke models have been reviewed by *Nucci et al.* [1990], *Thottappillil and Uman* [1993], *Thottappillil et al.* [1997], *Rakov and Uman* [1998], and *Gomes and Cooray* [2000].

[4] Distributed circuit models of the lightning return stroke usually consider the lightning channel as an *R-L-C* transmission line [e.g., *Mattos and Christopoulos*, 1988; *Baum and Baker*, 1990], where R, L, and C are series resistance, series inductance, and shunt capacitance, all per unit length, respectively. In an *R-L-C* transmission line model, voltage and current are the solutions of the telegrapher's equations. Note that the telegrapher's equations can be derived from Maxwell's equations assuming that the electromagnetic waves guided by the transmission line have a transverse electromagnetic (TEM) field structure. Strictly speaking, the latter assumption is not valid for a vertical conductor above ground. Indeed, any current wave suffers attenuation as it propagates upward along a vertical conductor, except for the special (unrealistic) case of a zero-radius vertical perfectly conducting wire excited at its bottom by an infinitesimal current source [*Thottappillil et al.*, 2001], and the resultant electromagnetic field structure is non-TEM [e.g., *Kordi et al.*, 2002, 2003a; *Baba and Rakov*, 2003, 2005b]. Clearly, an incorrect assumption on the electromagnetic field structure (e.g., TEM when it is actually non-TEM) in the vicinity of lightning channel will result in an incorrect current distribution along the channel (as discussed, for example, by *Baba and Rakov* [2003]).

[5] Electromagnetic return-stroke models are based on Maxwell's equations [*Rakov and Uman*, 1998]. These are relatively new and most rigorous (no TEM assumption) models suitable for specifying the source in studying lightning interaction with various systems and with the environment. In this class of models, Maxwell's equations are solved to yield the distribution of current along the lightning channel using numerical techniques, such as the method of moments (MoM) [*Harrington*, 1968; *Van Baricum and Miller*, 1972; *Miller et al.*, 1973] and the finite difference time domain (FDTD) method [*Yee*, 1966]. The resultant distribution of channel current can be used to compute electric and magnetic fields radiated by the lightning channel. In order to reduce the speed of current wave propagating along the channel-representing wire to a value lower than the speed of light in air, c, a wire is embedded in a dielectric (other than air) [e.g., *Moini et al.*, 1997, 2000] or loaded by additional distributed series inductance [e.g., *Kato et al.*, 1999]. Capacitive loading has been also suggested [*Bonyadi-ram et al.*, 2004]. In contrast with distributed-circuit and engineering models, electromagnetic return-stroke models allow a self-consistent full-wave solution for both lightning-current distribution and resultant electromagnetic fields. One of the advantages of the use of electromagnetic models, although it may be computationally expensive, is that one does not need to employ any model of field-to-conductor coupling in analyzing lightning-induced effects on electrical circuits [e.g., *Pokharel et al.*, 2003; *Tatematsu et al.*, 2004]. Electromagnetic models are generally capable of reproducing most salient features of observed electric and magnetic fields at distances ranging from tens of meters to hundreds of kilometers [e.g., *Moini et al.*, 2000; *Baba and Ishii*, 2003; *Shoory et al.*, 2005].

[6] The first peer-reviewed journal paper concerned with an electromagnetic model was published in 1987 [*Podgorski and Landt*, 1987], and more than a dozen of journal papers and a very large number of conference papers were published during the last seven years or so. The amount of published material on lightning electromagnetic models is presently such that the area is in need of consolidating review. Interest in using electromagnetic models continues to grow, in part because of availability of numerical codes and increased computer capabilities. At the same time certain aspects (or even the concept) of these models are misunderstood by some researchers and appear to be in need of clarification.

[7] In this paper, we classify electromagnetic models of the lightning return stroke, proposed or used as of today, in terms of the channel representation, the excitation method, and the employed numerical technique (or procedure). Additionally considered here is the so-called hybrid electromagnetic/circuit theory (HEM) model [*Visacro et al.*, 2002], which employs electric scalar and magnetic vector potentials for taking account of electromagnetic coupling but is formulated in terms of circuit quantities, voltages and currents. Since the HEM model, on the one hand, yields a non-TEM close electromagnetic field structure (as do electromagnetic models) and, on the other hand, apparently considers electric and magnetic fields as decoupled (as in distributed circuit models), it occupies an intermediate place between electromagnetic and distributed circuit models. We will show in this paper that its predictions are similar to those of electromagnetic models. Application of the HEM model to lightning return-stroke studies and to analyzing the interaction of lightning with grounded objects is described by *Visacro and Silveira* [2004] and by *Visacro and Soares* [2005], respectively.

[8] The structure of this paper is as follows. In section 2, we show that a current wave necessarily suffers attenuation (dispersion to be exact) as it propagates upward along a vertical non-zero-thickness wire above perfectly conducting ground excited at its bottom by a lumped source, even if the wire has no ohmic losses, which is a distinctive feature of electromagnetic return-stroke models. In section 3, we classify electromagnetic return-stroke models into four types depending on lightning channel representation used to find the distribution of current along the channel: a perfectly conducting or resistive wire in air, a wire embedded in a dielectric (other than air), a wire in air loaded by additional distributed series inductance, and two wires in air having additional distributed shunt capacitance. In section 4, we describe methods of excitation used in electromagnetic return-stroke models: closing a charged vertical wire at its bottom with a specified impedance (or circuit), a delta-gap electric field source, and a lumped current source. In section 5, we review representative numerical procedures for solving Maxwell's equations used in electromagnetic models of the lightning return stroke: MoMs in the time and frequency domains, and the FDTD method. In Appendix A,

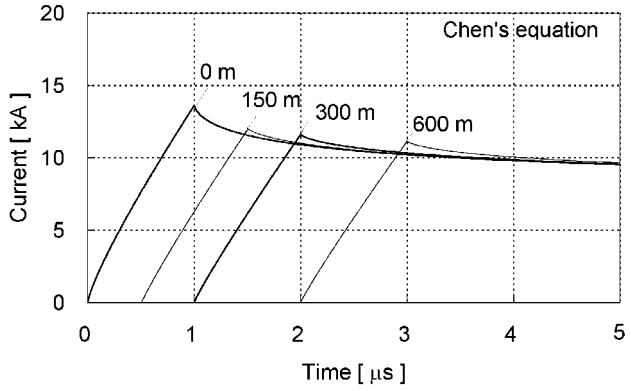

Figure 1. Current waveforms at different heights calculated using Chen's analytical equation (see (1)) for a vertical perfectly conducting cylinder of radius 0.23 m in air above perfectly conducting ground excited at its bottom by a zero-length voltage source. The source produces a ramp wave having a magnitude of 5 MV and a risetime of 1 μs.

we compare current distributions along a vertical wire calculated using an electromagnetic model with that calculated using the HEM model.

2. General Approach to Finding the Current Distribution Along a Vertical Perfectly Conducting Wire Above Ground

[9] All electromagnetic return-stroke models involve a representation of the lightning channel as a non-zero-thickness vertical wire. In this section, using *Chen*'s [1983] analytical equation, we show that a current wave necessarily suffers attenuation as it propagates along a vertical wire of uniform nonzero thickness that is located above perfectly conducting ground and excited at its bottom by a lumped source, even if the wire has no ohmic losses. This effect, generally known in the radio science community, but apparently not in the lightning research community [e.g., *Bermudez et al.*, 2003], is usually attributed to radiation losses. Here, we show that current attenuation (or, more generally, dispersion, to be understood here as changes in pulse waveshape) is necessary to satisfy the boundary condition on the tangential electric field on the surface of vertical wire.

2.1. Current Distribution Along a Vertical Perfectly Conducting Wire Above Ground

[10] *Chen* [1983] has derived an approximate analytical equation for the transient current $I(z', t)$ along an infinitely long perfectly conducting cylinder in air excited in the middle by a zero-length voltage source generating step voltage V. This equation is reproduced below.

$$I(z',t) = \frac{2V}{\eta}\tan^{-1}\left(\frac{\pi}{2\ln\left(\sqrt{c^2t^2 - z'^2}/a\right)}\right), \qquad (1)$$

where η is free space impedance (120π Ω), ln is the natural logarithm, and a is the radius of the cylinder. Note that Chen's equation (1) yields results that are almost identical to those given by exact formula of *Wu* [1961]. If we apply (1) to a vertical cylinder on flat perfectly conducting ground excited at its bottom by a zero-length step-voltage source, we have only to multiply the magnitude of resultant current by 2 in order to account for the image source. Chen's analytical equation (1) can be used in testing the accuracy of numerical techniques employed in electromagnetic models of the lightning return stroke.

[11] Figure 1 shows current waveforms at different heights along a vertical perfectly conducting wire of radius 0.23 m in air above ground excited at its bottom by a zero-length source that produces a ramp-front wave having a magnitude of 5 MV and a risetime of 1 μs. Note that we obtained the response to this ramp-front voltage wave using numerical convolution since (1) is the solution for a step voltage excitation.

[12] It is clear from Figure 1 that a current wave suffers attenuation as it propagates along the vertical perfectly conducting wire above ground. We will show in section 5.3 that current waveforms calculated using the MoM in the time and frequency domains and the FDTD method agree well with those calculated using Chen's equation.

2.2. Mechanism of Attenuation of Current Wave in the Absence of Ohmic Losses

[13] According to analytical equation (1), any current wave suffers attenuation as it propagates upward along a vertical perfectly conducting wire above flat perfectly conducting ground excited at its bottom by a lumped source (the same result follows from numerical solution of Maxwell's equations [e.g., *Kordi et al.*, 2002, 2003a; *Baba and Rakov*, 2003, 2005b]), except for the ideal (unrealistic) case of a zero-thickness wire excited by a zero-length source [*Thottappillil et al.*, 2001]. In this section, we discuss the mechanism of current attenuation in the absence of ohmic losses.

[14] *Baba and Rakov* [2005b] visualized the mechanism of attenuation of current wave propagating along a vertical non-zero-thickness perfectly conducting wire as illustrated in Figure 2. A reference (no interaction with the wire, no attenuation) positive current pulse I_{inc} propagating upward generates an incident spherical TEM wave [*Thottappillil et al.*, 2001], with vertical electric field component on the surface of the wire being directed downward. Cancellation of this field, as required by the boundary condition on the tangential electric field on the surface of a perfectly conducting wire, gives rise to an induced or "scattered" current I_{scat}. This scattered current I_{scat} modifies I_{inc}, so that the resultant total current pulse I_{tot} appears attenuated as it propagates along the vertical wire. The attenuation of the total current pulse is accompanied by the lengthening of its tail, such that the total charge transfer is independent of height. The electromagnetic field structure associated with an attenuated current distribution along a vertical wire is non-TEM. *Baba and Rakov* [2005b] have shown that the current attenuation becomes more pronounced as (1) the thickness of vertical wire increases, (2) the source height decreases, (3) the frequency increases, and (4) the height above the excitation point decreases.

[15] In summary, current attenuation (or, more generally, dispersion) is necessary to satisfy the boundary condition on the tangential electric field on the surface of vertical wire.

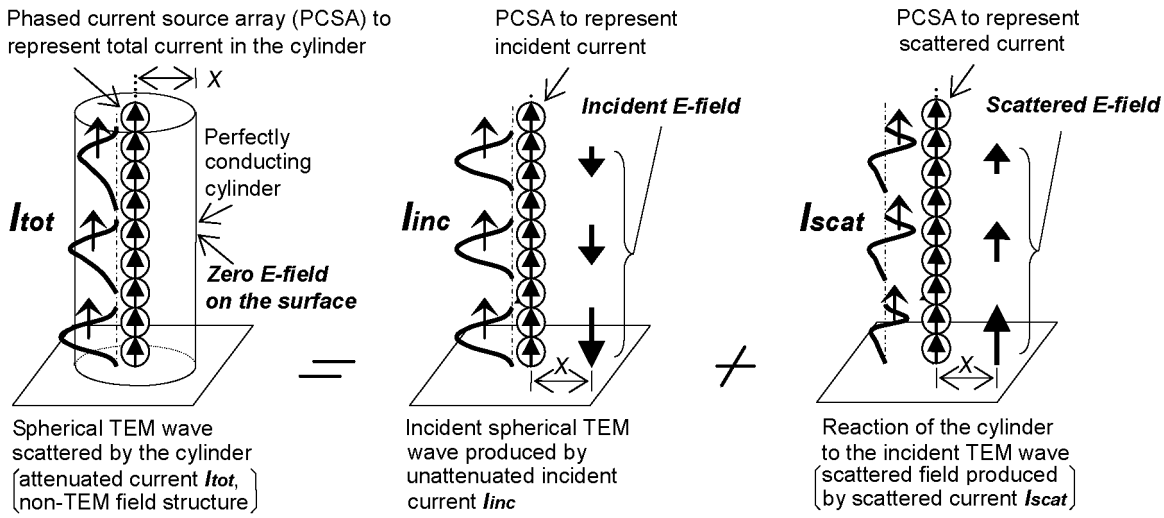

Figure 2. Conceptual picture to explain the mechanism of current attenuation along a vertical non-zero-thickness perfectly conducting wire above perfectly conducting ground. All currents are assumed to flow on the axis. An attenuated "total" current pulse I_{tot} is separated into an "incident" unattenuated current pulse I_{inc} and an induced or "scattered" current pulse I_{scat}. I_{inc} generates an incident downward vertical electric field at a horizontal distance x from the axis (on the lateral surface of the cylinder). I_{scat} produces a scattered upward vertical electric field that cancels the incident downward vertical electric field on the surface of the cylinder and modifies the incident current I_{inc}. The resultant current pulse, $I_{tot} = I_{inc} + I_{scat}$, appears attenuated, and its tail is lengthened as this pulse propagates along the wire. Adapted from *Baba and Rakov* [2005b] (© 2005 IEEE).

The resultant field structure is non-TEM, particularly in the vicinity of the excitation point.

3. Representation of the Lightning Return Stroke Channel

[16] In this section, we classify electromagnetic return-stroke models into four types depending on channel representation: (1) a perfectly conducting/resistive wire in air above ground, (2) a wire embedded in a dielectric (other than air) above ground, (3) a wire loaded by additional distributed series inductance in air above ground, and (4) two wires having additional distributed shunt capacitance in air.

[17] Representations 2, 3, and 4 are used to reduce the speed of current wave propagating along the channel-representing wire to a value lower than the speed of light in air. Table 1 gives a list of papers on electromagnetic models of the lightning return stroke that are grouped into four categories depending on the channel representation.

[18] Two features of the lightning return stroke to be reproduced by models are as follows: (1) Typical values of return-stroke wavefront speed are in the range from $c/3$ to $2c/3$ [e.g., *Rakov*, 2004], as observed using optical techniques. (2) The equivalent impedance of the lightning return-stroke channel is expected to be in the range from 0.6 to 2.5 kΩ [*Gorin and Shkilev*, 1984], as estimated from measurements of lightning current at different points along the 540-m-high Ostankino Tower in Moscow.

[19] Values of the radius of lightning channel in Table 1 are larger than expected [e.g., *Rakov*, 1998], but this is much less important than agreement of the characteristic impedance of the simulated channel with expected equivalent channel impedance values (0.6 to 2.5 kΩ).

[20] Note that the resistance per unit length of a lightning return-stroke channel (behind the return-stroke front) is estimated to be about 0.035 Ω/m and about 3.5 Ω/m ahead of the return-stroke front [*Rakov*, 1998]. Values of distributed resistance (for the case of resistive channel) in Table 1 are between these two expected values.

3.1. Perfectly Conducting/Resistive Wire in Air Above Ground

[21] In this section, we discuss the representation of the lightning return-stroke channel as a vertical perfectly conducting or resistive wire in air above ground. The channel-representing wire is excited at its termination point (ground level or the top of a grounded strike object) by a delta-gap electric field source. A lumped current source is not suitable for modeling of the lightning return stroke when it terminates on a tall grounded object [*Baba and Rakov*, 2005a].

[22] The resultant speed of current wave propagating along such a vertical wire is essentially equal to the speed of light, which is 1.5 to 2 times larger than typical measured values of return stroke wavefront speed: $c/3$ to $2c/3$ [e.g., *Rakov*, 2004]. The characteristic impedance of the wire (e.g., 400 to 700 Ω for a 50-mm-radius vertical perfectly conducting wire [*Baba and Ishii*, 2003]) is somewhat lower than the equivalent impedance of the natural lightning return-stroke channel (0.6 to 2.5 kΩ [*Gorin and Shkilev*, 1984]). As shown in section 2, a current wave suffers attenuation as it propagates along a vertical wire even if it has no ohmic losses. Additional distributed series resistance causes further attenuation, which can be used to control this effect.

[23] *Podgorski and Landt* [1987] and *Podgorski* [1991], using the modified Thin-Wire Time Domain (TWTD) code

Table 1. List of Papers on Electromagnetic Models of the Lightning Return Stroke Grouped Into Four Categories Depending on the Lightning Channel Representation[a]

Papers	Channel Radius, mm	ε_r	R, Ω/m	L, μH/m	C, pF/m	Phase Velocity
		Perfectly Conducting or Resistive Wire Above Ground				
Reviewed journal papers						
Podgorski and Landt [1987]	unknown	1	0.7	0	. . .	c
Kordi et al. [2002]	50	1	0	0	. . .	c
Mozumi et al. [2003]	100	1	0	0	. . .	c
Baba and Ishii [2003]	50	1	0, 0.1	0	. . .	c
Kordi et al. [2003b]	100	1	0.07	0	. . .	c
Baba and Rakov [2003, 2005b]	230, 2000[b]	1	0	0	. . .	c
Pokharel et al. [2004]	100	1	0.1	0	. . .	c
Other publications						
Podgorski [1991]	unknown	1	0.7	0	. . .	c
Chai et al. [1994]	500	1	unknown	0	. . .	c
Kato et al. [2001]	10	1	0	0	. . .	c
Kordi et al. [2003a]	50	1	0	0	. . .	c
Grcev et al. [2003]	100	1	0	0	. . .	c
Maslowski [2004]	unknown	1	1	0	. . .	c
		Wire Above Ground Embedded in Dielectric of $\varepsilon_r > 1$				
Reviewed journal papers						
Moini et al. [1998, 2000]	unknown	4, 5.3	0, 0.07	0	. . .	0.5c, 0.43c
Shoory et al. [2005]	50	5.3	0.1	0	. . .	0.43c
Other publications						
Moini et al. [1997]	unknown	5.3	0.1	0	. . .	0.43c
Kato et al. [2001]	10	200 (4-m coating)	0	0	. . .	0.7c
Grcev et al. [2003]	10	5.3	0	0	. . .	0.43c
		Wire Above Ground Loaded by Distributed Series Inductance				
Reviewed journal papers						
Baba and Ishii [2001, 2003]	300, 50	1	1	3, 6	. . .	0.56c, 0.43c
Pokharel et al. [2003, 2004]	10, 100	1	0.5, 1	6, 9	. . .	0.43c, 0.37c
Other publications						
Kato et al. [1999, 2001]	10	1	0	0.1, 2.5	. . .	0.33c, 0.7c
Aniserowicz [2004]	50	1	1	4.5 to 7.5	. . .	0.43c
Bonyadi-ram et al. [2004]	20	1	0.3	8	. . .	0.43c
Miyazaki and Ishii [2004, 2005]	unknown	1	1	3	. . .	0.5c
Tatematsu et al. [2004]	460	1	0	1.5, 10	. . .	0.6c, 0.31c
Petrache et al. [2005]	100	1	1	3	. . .	0.5c
Noda et al. [2005]	230	1	0	10	. . .	0.33c
		Wire Loaded by Distributed Shunt Capacitance				
Reviewed journal papers						
None						
Other publications						
Bonyadi-ram et al. [2005]	20	1	0.2	0	50	0.43c

[a] R, L, and C are the additional resistance, inductance, and capacitance (each per unit length), respectively, of the equivalent lightning channel.
[b] 2 m × 2 m rectangular cross section.

[*Van Baricum and Miller*, 1972], have represented a lightning strike to the 553-m-high CN Tower in Toronto by a precharged resistive (0.7 Ω/m) vertical wire having nonlinear resistance (10 kΩ prior to the attachment and 3 Ω after the attachment) at its termination point at the top of the CN Tower.

[24] The main deficiency of this channel representation is the unrealistic current wave propagation speed equal to the speed of light. This should result in overestimation of remote electric and magnetic fields, since their magnitudes are expected to be proportional to the current wave propagation speed [e.g., *Uman et al.*, 1975; *Rakov and Dulzon*, 1987].

3.2. Wire Embedded in a Dielectric (Other Than Air) Above Ground

[25] In this section, we first review the TEM-wave-based *R-L-C* uniform transmission line theory, and then, on the basis of this theory, discuss the representation of lightning return-stroke channel using a vertical wire embedded in a dielectric. Note that applying the *R-L-C* transmission-line theory to describing a vertical wire above ground is an

approximation, since inductance L and capacitance C, both per unit length, vary with height along the vertical wire, and the resultant electromagnetic field structure is non-TEM.

[26] The propagation constant γ_0 of the *R-L-C* uniform transmission line, the phase velocity v_{p0} of a wave propagating along this line, and the characteristic impedance Z_{c0} of the line are given by [e.g., *Sadiku*, 1994; *Rakov*, 1998],

$$\gamma_0 = \sqrt{j\omega C_0 (R_0 + j\omega L_0)}, \tag{2}$$

$$v_{p0} = \frac{\omega}{\mathrm{Im}(\gamma_0)} = \frac{1}{\sqrt{L_0 C_0}} \left[\frac{2}{\sqrt{1 + (R_0/\omega L_0)^2} + 1} \right]^{1/2}, \tag{3}$$

$$Z_{c0} = \sqrt{\frac{R_0 + j\omega L_0}{j\omega C_0}}, \tag{4}$$

where $\mathrm{Im}\{\gamma_0\}$ stands for the imaginary part of γ_0, ω is the angular frequency ($2\pi f$), R_0 is the series resistance per unit length, L_0 is the natural series inductance per unit length, and C_0 is the natural shunt capacitance per unit length. If ωL_0 is much larger than R_0 at a frequency of interest, (3) and (4) reduce to

$$v_{p0} \simeq 1/\sqrt{L_0 C_0}, \tag{5}$$

$$Z_{c0} \simeq \sqrt{L_0/C_0}. \tag{6}$$

The assumption that (5) and (6) are based on is satisfied at frequencies f = 1 MHz or higher for L_0 = 2.1 μH/m (evaluated for a 30-mm-radius horizontal wire at a height of 500 m above ground [*Rakov*, 1998]) and R_0 = 1 Ω/m, where ωL_0 (= 13 Ω/m) $\gg R_0$ (= 1 Ω/m). If the transmission line is surrounded by air, v_{p0} given by (5) is equal to c. When a vertical wire is embedded in a dielectric of ε_r, the phase velocity v_{pd} and the characteristic impedance Z_{cd} for this wire become

$$v_{pd} \simeq \frac{1}{\sqrt{L_0\, \varepsilon_r C_0}} = \frac{v_{p0}}{\sqrt{\varepsilon_r}} = \frac{c}{\sqrt{\varepsilon_r}}, \tag{7}$$

$$Z_{cd} \simeq \sqrt{\frac{L_0}{\varepsilon_r C_0}} = \frac{Z_{c0}}{\sqrt{\varepsilon_r}} = \frac{v_{pd}}{c}\, Z_{c0}. \tag{8}$$

Equations (7) and (8) show that, in this representation, Z_{cd} decreases linearly with decreasing v_{pd}, although it is unknown if this trend will hold for an actual lighting return stroke.

[27] When ε_r ranges from 2.25 to 9, v_{pd} ranges from 0.67c to 0.33c, which corresponds to typical measured speeds of the lightning return-stroke wavefront [e.g., *Rakov*, 2004]. The corresponding characteristic impedance Z_{cd} ranges from 0.13 to 0.27 kΩ for v_{pd} = 0.33c, and 0.23 to 0.47 kΩ for v_{pd} = 0.67c, respectively, if the characteristic impedance of a vertical nonloaded wire in air ranges from Z_{c0} = 0.4 to 0.7 kΩ ($v_{p0} = c$) [*Baba and Ishii*, 2003]. This characteristic impedance (Z_{cd} = 0.13 to 0.47 kΩ) is smaller than values of the expected equivalent impedance of the lightning return stroke channel (0.6 to 2.5 kΩ) [*Gorin and Shkilev*, 1984]. However, it does not cause significant differences in resultant current distributions in analyzing a branchless subsequent lightning stroke terminating on flat ground, in which upward connecting leaders are usually neglected and the return-stroke current wave propagates upward from the ground surface. However, in analyzing lightning strikes to a grounded metallic object using this representation, one needs to insert several-hundred-ohm lumped resistance between the lightning channel and the strike object in order to obtain a realistic impedance of the lightning return-stroke channel seen by waves entering the channel from the strike object. This will be illustrated in section 3.5.

[28] *Moini et al.* [1998, 2000], *Grcev et al.* [2003], and *Shoory et al.* [2005] have represented a lightning return-stroke channel by a vertical perfectly conducting or resistive wire excited at its bottom by a delta-gap electric field source or a lumped current source on flat conducting ground. In finding the distribution of current along this wire, they assumed ε_r = 5.3 [*Moini et al.*, 2000; *Grcev et al.*, 2003; *Shoory et al.*, 2005] or 4 [*Moini et al.*, 1998] in order to reduce the speed of current wave propagating along the wire to a value lower than the speed of light c (0.43c or $0.5c = c/\sqrt{\varepsilon_r}$, respectively). The surrounding dielectric was intended to account for the effect of corona capacitance (via increasing ε_r) and was assumed to occupy the entire half-space above the perfectly conducting ground. *Moini et al.* [2000] and *Shoory et al.* [2005] tested their return-stroke model by comparing the model-predicted electric and magnetic fields 0.5, 5, and 100 km from the lightning channel with the corresponding fields measured by *Lin et al.* [1979]. Note that the fields were calculated assuming the wire was surrounded by air (ε_r = 1) and using the distribution of current along the wire found for ε_r = 5.3. This approach was also employed by *Moini et al.* [1998] in calculating lightning-induced voltages on overhead wires above perfectly conducting ground. *Moini et al.* [1998, 2000] used the MoM in the time domain, while *Grcev et al.* [2003] and *Shoory et al.* [2005] used the MoM in the frequency domain. *Shoory et al.* [2005] considered finitely conducting ground.

[29] *Aniserowicz* [2004] has found a useful relation between a resistive wire loaded by additional distributed series inductance and a resistive wire embedded in a dielectric. From (2), the propagation constant for a resistive transmission line embedded in a dielectric of relative permittivity ε_r is given by

$$\gamma_d = \sqrt{j\omega\, \varepsilon_r\, C_0\, (R_0 + j\omega L_0)}, \tag{9}$$

which can be written as

$$\gamma_i = \sqrt{j\omega\, C_0\, (\varepsilon_r R_0 + j\omega \varepsilon_r L_0)}. \tag{10}$$

Equations (9) and (10) show that the effect of distributed resistance $\varepsilon_r R_0$ (= 5.3 R_0) of a wire in air loaded by additional

distributed series inductance $L = (\varepsilon_r - 1)\, L_0$ (=4.3 L_0) on the propagation constant is the same as that of R_0 of a wire embedded in a dielectric of relative permittivity ε_r (=5.3). For example, the effect of $R_0 = 0.07\ \Omega$/m of a wire embedded in a dielectric of $\varepsilon_r = 5.3$ [e.g., *Moini et al.*, 2000] on the propagation constant is the same as that of $\varepsilon_r R_0 = 0.37\ \Omega$/m of a wire in air loaded by $L = 4.3\ L_0$.

[30] It follows from (3) that the phase velocity v_{pi} for a wire surrounded by air having a distributed series resistance $\varepsilon_r R_0$ and an additional distributed series inductance $L = (\varepsilon_r - 1)L_0$ is the same as the phase velocity v_{pd} for a wire having a distributed series resistance R_0 and being embedded in a dielectric of ε_r. The characteristic impedances of these two wires are given respectively by

$$Z_{ci} = \sqrt{\frac{\varepsilon_r R_0 + j\omega\varepsilon_r L_0}{j\omega C_0}} = \sqrt{\varepsilon_r} Z_{c0}, \tag{11}$$

$$Z_{cd} = \sqrt{\frac{R_0 + j\omega L_0}{j\omega\varepsilon_r C_0}} = \frac{Z_{c0}}{\sqrt{\varepsilon_r}} = \frac{Z_{ci}}{\varepsilon_r}. \tag{12}$$

Equations (11) and (12) show that the effect of distributed resistance $\varepsilon_r R_0$ of a wire in air loaded by an additional distributed series inductance $L = (\varepsilon_r - 1)L_0$ on the characteristic impedance, relative to that of total inductance $\varepsilon_r L_0$, is the same as that of R_0 of a wire embedded in a dielectric of relative permittivity ε_r, relative to that of natural inductance L_0.

[31] *Kato et al.* [2001] have represented the lightning return-stroke channel by a vertical perfectly conducting wire, which is placed along the axis of a 4-m-radius dielectric cylinder of $\varepsilon_r = 200$ and excited at its bottom by a delta-gap electric field source. This dielectric cylinder was surrounded by air ($\varepsilon_r = 1$). The resultant speed of current wave propagating along this wire was about $0.7c$. Note that a conductor with dielectric coating is known as the Goubau waveguide [*Goubau*, 1950].

[32] Clearly, the use of artificial dielectric creates a discontinuity in computing lightning electric and magnetic fields. Also, it can potentially influence the distribution of current along the lightning channel and resultant remote fields, although this influence is expected to be small [e.g., *Moini et al.*, 2000].

3.3. Wire Loaded by Additional Distributed Series Inductance in Air Above Ground

[33] In this section, as done in section 3.2, we use (5) and (6), which are based on the *R-L-C* uniform transmission line approximation, to examine parameters of a vertical wire loaded by additional distributed series inductance L in air. From (5) and (6), the phase velocity v_{pi} and the characteristic impedance Z_{ci} for such a wire are

$$v_{pi} \simeq \frac{1}{\sqrt{(L_0 + L)\, C_0}} = \sqrt{\frac{L_0}{L_0 + L}}\, v_{p0} = \sqrt{\frac{L_0}{L_0 + L}}\, c, \tag{13}$$

$$Z_{ci} \simeq \sqrt{\frac{L_0 + L}{C_0}} = \sqrt{\frac{L_0 + L}{L_0}}\, Z_{c0} = \frac{c}{v_{pi}}\, Z_{c0}. \tag{14}$$

Equations (13) and (14) show that if $L = 3L_0$, v_{pi} becomes $0.5c$ and Z_{ci} becomes $2Z_{c0}$. In this representation, Z_{ci} increases linearly with decreasing v_{pi}. Note that additional inductance has no physical meaning and is invoked only to reduce the speed of current wave propagating along the wire to a value lower than the speed of light. Electromagnetic waves radiated from the vertical inductance-loaded wire into air propagate at the speed of light. The use of this representation allows one to calculate both the distribution of current along the channel-representing wire and the radiated electromagnetic waves in a single, self-consistent procedure, while that of a vertical wire embedded in a dielectric described in section 3.2 requires two steps to achieve the same objective.

[34] If the natural inductance of a vertical wire is assumed to be $L_0 = 2.1\ \mu$H/m (evaluated as for a 30-mm-radius horizontal wire at a height of 500 m above ground by *Rakov* [1998]), the additional inductance needed to simulate $v_{pi} = 0.67c$ and $0.33c$ is estimated from (13) to be $L = 2.6$ and 17 μH/m, respectively. As noted above, typical measured speed of natural lightning return-stroke wavefront ranges from $0.33c$ to $0.67c$ [e.g., *Rakov*, 2004]. These inductance values (2.6 and 17 μH/m) are not much different from those employed to date, which range from 1.5 [*Tatematsu et al.*, 2004] to 10 μH/m [*Noda et al.*, 2005; *Tatematsu et al.*, 2004], except for that employed by *Kato et al.* [1999], who used 0.1-μH/m additional inductance. The resultant speeds of current waves propagating along the wire are about $0.6c$ and $0.3c$ for the wire loaded by $L = 1.5$ and 10 μH/m, respectively, and $0.33c$ for 0.1 μH/m. In summary, in order to simulate a typical speed of return-stroke wavefront, appropriate values of additional distributed inductance should be selected to be roughly from 1 to 20 μH/m.

[35] From (14), Z_{ci} ranges from 0.6 to 1.0 kΩ for $v_{pi} = 0.67c$, and 1.2 to 2.1 kΩ for $v_{pi} = 0.33c$, respectively, if the characteristic impedance of a vertical wire without inductive loading ranges from 0.4 to 0.7 kΩ ($v_{p0} = c$) [*Baba and Ishii*, 2003]. The characteristic impedance of the inductance-loaded wire (Z_{ci} = 0.6 to 2.1 kΩ) is consistent with the expected values of equivalent impedance of the lightning return stroke (ranging from 0.6 to 2.5 kΩ [*Gorin and Shkilev*, 1984]). Note that the equivalent impedance of a 50-mm-radius vertical wire loaded by 3- or 6-μH/m additional distributed series inductance and 1-Ω/m distributed series resistance is 0.7 to 2.0 kΩ or 0.9 to 2.0 kΩ for the current-wave propagation speed of $0.56c$ or $0.43c$, respectively [*Baba and Ishii*, 2003]. This is within the range of values of the expected equivalent impedance of the lightning return-stroke channel.

[36] *Baba and Ishii* [2001, 2003] added distributed series resistance of 1 Ω/m to an inductance-loaded wire in order to stabilize nonphysical oscillations caused by the employed numerical procedure. This same resistance value was also used by *Aniserowicz* [2004], *Miyazaki and Ishii* [2004, 2005], *Petrache et al.* [2005], and *Pokharel et al.* [2004].

3.4. Two Wires Having Additional Distributed Shunt Capacitance in Air

[37] In this section, as done in sections 3.2 and 3.3, we use (5) and (6) to examine parameters of a wire having additional distributed shunt capacitance in air. From (5) and (6), the

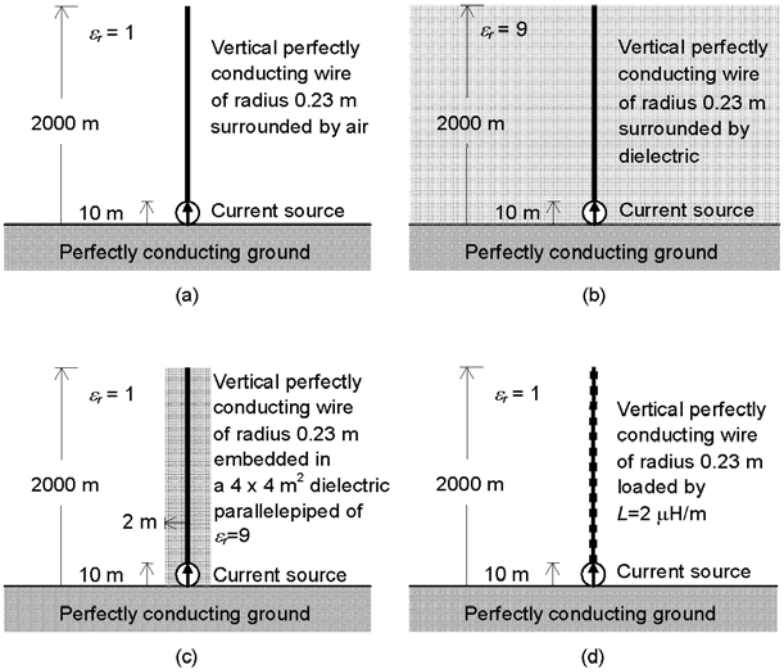

Figure 3. Four representations of lightning return stroke channel above flat perfectly conducting ground excited at its bottom by a 10-m current source: (a) a 0.23-m-radius vertical perfectly conducting wire surrounded by air, (b) a 0.23-m-radius vertical perfectly conducting wire surrounded by dielectric (ε_r = 9), (c) a 0.23-m-radius vertical perfectly conducting wire embedded in a 4 × 4 m^2 dielectric parallelepiped of ε_r = 9 surrounded by air, and (d) a 0.23-m-radius vertical perfectly conducting wire having additional distributed series inductance L = 2 μH/m in air.

phase velocity v_{pc} and the characteristic impedance Z_{cc} for this case are given by

$$v_{pc} \simeq \frac{1}{\sqrt{L_0(C_0 + C)}} = \sqrt{\frac{C_0}{C_0 + C}}\, v_{p0} = \sqrt{\frac{C_0}{C_0 + C}}\, c, \quad (15)$$

$$Z_{cp} \simeq \sqrt{\frac{L_0}{C_0 + C}} = \sqrt{\frac{C_0}{C_0 + C}}\, Z_{c0} = \frac{v_{pc}}{c}\, Z_{c0}. \quad (16)$$

[38] *Bonyadi-ram et al.* [2005] evaluated the distribution of current along a lightning return stroke channel approximating this channel and its image by two 7-km-long parallel wires, which had additional shunt capacitance and were excited at their one end by a delta-gap electric field source. Each wire had a radius of 20 mm, and the separation between the wires was 30 m. The resultant parallel-wire transmission line had a distributed series resistance of 0.2 Ω/m. The additional shunt capacitance was C = 50 pF/m, which allowed them to reduce the speed of current wave propagating along the parallel wires to $v = 0.43c$. The current distribution, obtained for the two capacitively loaded parallel wires was used to calculate electric and magnetic fields 0.5, 5, and 100 km from a vertical lightning channel above ground. The approach of *Bonyadi-ram et al.* [2005] is somewhat similar to that of *Moini et al.* [1997, 2000]: the use of a fictitious configuration for finding a reasonable distribution of current along the lightning channel and then application of this current distribution to the actual configuration (vertical wire in air above ground).

3.5. Comparison of Distributions of Current for Different Channel Representations

[39] In this section, we compare distributions of current along a vertical channel above perfectly conducting ground excited at its bottom by a lumped current source that are predicted by different models. Further, we show effects of distributed series resistance, relative permittivity of surrounding dielectric, and additional distributed series inductance on the speed of current waves.

[40] Figure 3 shows four representations of lightning return stroke channel above flat perfectly conducting ground by a vertical perfectly conducting wire of radius 0.23 m in air (Figure 3a), a vertical perfectly conducting wire of radius 0.23 m embedded in dielectric of ε_r = 9, which occupies the entire half-space (Figure 3b), a vertical perfectly conducting wire of radius 0.23 m embedded in a 4 × 4 m^2 dielectric parallelepiped of ε_r = 9 surrounded by air (Figure 3c), and a vertical perfectly conducting wire of radius 0.23 m in air loaded by additional distributed series inductance L = 2 μH/m (Figure 3d). In all four cases the wire is excited at its bottom by a 10-m-long lumped current source. The lumped current source produces the channel-base (z' = 0) current waveform shown in Figure 1.

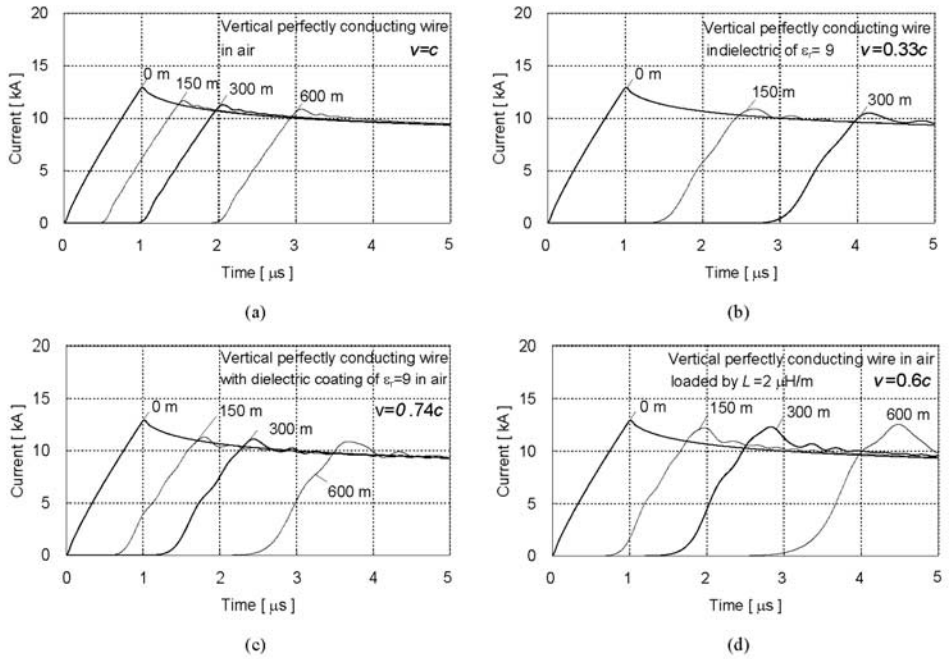

Figure 4. Current waveforms at different heights calculated using the FDTD method for four representations of the lightning return stroke channel shown in Figures 3a–3d. In the FDTD calculations, the vertical perfectly conducting wire is represented by a zero-radius wire placed in the working volume of $60 \times 60 \times 2300$ m^3, which is divided into $1 \times 1 \times 10$ m^3 cells. When cells having a cross-sectional area of 1 m $\times$ 1 m are used and no modification is made for relative permittivity and permeability of medium surrounding the wire, the vertical (z-directed) zero-radius perfectly conducting wire in air has an equivalent radius of 0.23 m [*Noda and Yokoyama*, 2002].

[41] Calculations were carried out using the FDTD method. For the FDTD calculations, the vertical perfectly conducting wire was represented by a zero-radius wire placed in the working volume of $60 \times 60 \times 2300$ m^3, which was divided into $1 \times 1 \times 10$ m^3 cells. When cells having a cross-sectional area of 1 m $\times$ 1 m are used and no modification is made for relative permittivity and permeability of medium surrounding the wire, the vertical (z-directed) zero-radius perfectly conducting wire in air has an equivalent radius of 0.23 m [*Noda and Yokoyama*, 2002]. Perfectly matched layers (PML) [*Berenger*, 1994] (absorbing boundaries) were set at the top and sides of the working volume in order to avoid reflections there. The time increment was set at 2 ns.

[42] Figure 4 shows distributions of current along the lightning return-stroke channel for its different representations shown in Figure 3, calculated using the FDTD method. It is clear from Figure 4a that a current wave propagates along the perfectly conducting wire in air at the speed of light. Figure 4b shows that a current wave propagates along the perfectly conducting wire surrounded by dielectric of $\varepsilon_r = 9$ at speed $v = 0.33c$, which is equal to $c/\sqrt{\varepsilon_r}$. Figure 4c shows that a current wave propagates along the perfectly conducting wire embedded in a 4×4 m^2 dielectric parallelepiped of $\varepsilon_r = 9$ surrounded by air at speed $v = 0.74c$. This is more than twice larger than in the case of the wire embedded in a dielectric which has the same permittivity and occupies the entire half-space (see Figure 4b). Figure 4d shows that a current wave propagates along the perfectly conducting wire in air loaded by additional distributed series inductance $L = 2$ μH/m at speed $v = 0.60c$.

[43] Table 2 summarizes speeds of current waves propagating along a vertical perfectly conducting wire embedded in a dielectric parallelepiped surrounded by air depending on the relative permittivity and thickness of the dielectric. Table 3 summarizes speeds of current waves propagating along a vertical perfectly conducting wire in air loaded by additional distributed series inductance depending on the value of added inductance. These speeds were calculated on the basis of times needed for current waves to propagate from $z' = 0$ to 300 m along the wire, which were determined by tracking an intersection point between a straight line passing through 10 and 90% points on the rising part of the current waveform and the time axis. It is clear from Table 2 that the current-wave-propagation speed decreases with increasing the thickness of dielectric coating and its relative permittivity, but the dependency is weak. For example, doubling the thickness of dielectric coating results in only

Table 2. Speed of Current Waves Propagating Along a 0.23-m-Radius Vertical Perfectly Conducting Wire Embedded in a Dielectric Parallelepiped Surrounded by Air as a Function of Relative Permittivity ε_r and Thickness of the Dielectric Layer

	Dielectric Constant ε_r	
Outer Dimensions of Dielectric	9	50
4×4 m^2	0.74c	0.68c
8×8 m^2	0.67c	0.59c
Upper half-space	0.33c	0.14c

Table 3. Speed of Current Waves Propagating Along a Vertical Perfectly Conducting Wire in Air Loaded by Additional Distributed Series Inductance as a Function of Added Inductance L

L, μH/m	v
2	0.60c
4	0.48c
8	0.37c

about 10% decrease in the current-wave-propagation speed, and an increase in the relative permittivity from $\varepsilon_r = 9$ to 50 also results in only about 10% decrease. In order to reduce the speed of current wave propagating along a vertical conducting wire having a dielectric coating, which is surrounded by air, to a value less than the speed of light, the relative permittivity of the dielectric coating needs to be much higher than the value that follows from $c/\sqrt{\varepsilon_r}$. It is clear from Table 3 that the current-wave-propagation speed decreases with increasing the value of added inductance.

[44] Figure 5 shows waveforms of current at heights of 0 and 300 m calculated using the FDTD method for a 0.23-m-radius vertical wire with or without resistive loading, surrounded by air above flat perfectly conducting ground and excited at its bottom by a 10-m-long current source. As the value of the added distributed series resistance, R, increases, attenuation and dispersion of current wave become larger. The speed of current wave, evaluated on the basis of the above definition, is essentially the same as the speed of light (when the distributed series resistance is larger than 2 Ω/m, current-wave-propagation speeds become higher than c because of the convex shape of current rising part). If we define the arrival time of current wave at $z' = 300$ m as the time when current at that height reaches 0.1 kA (threshold), speed values are always less than c. These are given in Table 4. When the value of distributed series resistance is larger than 1 to 2 Ω/m, the apparent speed of current waves propagating along the resistive wire decreases more appreciably with increasing R.

[45] We now discuss representation of the lightning channel in the presence of a tall strike object. Figure 6 shows a lightning strike to a 200-m-high grounded object. The lightning return-stroke channel is represented by a 0.23-m-radius vertical perfectly conducting wire embedded in a 4×4 m^2 dielectric of $\varepsilon_r = 9$ in air. The speed of current waves propagating along this channel-representing wire is 0.74c (see Table 2), and therefore the characteristic impedance is about 350 Ω (≈0.74 × 500 Ω) if the characteristic impedance of the wire without dielectric coating is assumed to be 500 Ω. This characteristic impedance (350 Ω) is lower than the expected equivalent impedance of the lightning channel, which ranges from 0.6 to 2.5 kΩ. The strike object is represented by a 0.23-m-radius vertical perfectly conducting wire. These two wires are excited at their connection point by a 10-m-long delta-gap electric field source in series with a lumped resistor of 0 or 500 Ω. We will examine the influence of this resistor on current waveforms at different heights along the channel. Figure 7 shows current waveforms at the top of the strike object (200 m above ground surface) and 400 m above the top of the object (600 m above ground surface) calculated using the FDTD method. It is clear from Figure 7 that both the shape and amplitude of current wave propagating along the channel are significantly influenced by

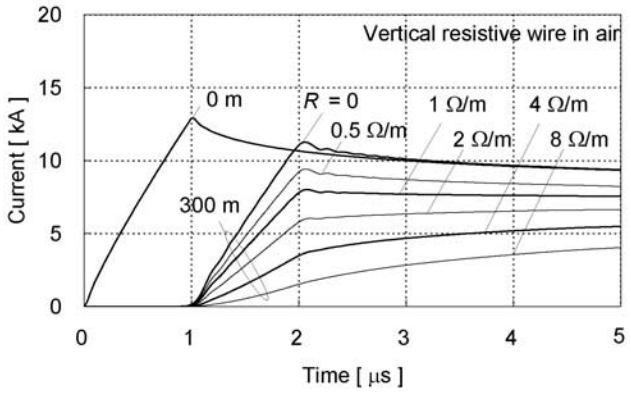

Figure 5. Current waveforms at heights of 0 and 300 m calculated using the FDTD method for a 0.23-m-radius vertical wire with or without resistive loading surrounded by air above flat perfectly conducting ground and excited at its bottom by a 10-m-long current source.

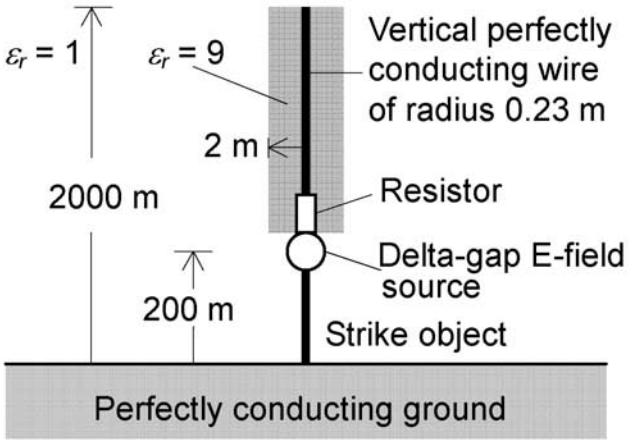

Figure 6. Lightning strike to a 200-m-high grounded object. The lightning return-stroke channel is represented by a 0.23-m-radius vertical perfectly conducting wire embedded in a 4×4 m^2 dielectric parallelepiped of $\varepsilon_r = 9$ in air and the strike object is represented by a 0.23-m-radius vertical perfectly conducting wire in air. A 10-m-long delta-gap electric field source is inserted at the connection point of these wires and in series with a lumped resistor (0 or 500 Ω). This source produces a ramp-front wave having a magnitude of 500 kV/m (5 MV along the 10-m-long source) and a risetime of 1 μs.

Table 4. Apparent Speed of Current Waves Propagating Along a Vertical Resistive Wire in Air as a Function of Distributed Series Resistance R

R, Ω/m	v
0	c
0.5	0.99c
1	0.99c
2	0.97c
4	0.93c
8	0.85c

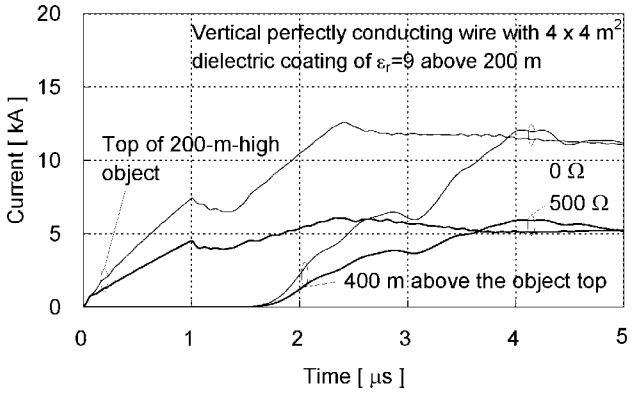

Figure 7. Current waveforms at different heights calculated using the FDTD method for the configuration shown in Figure 6.

the presence of the lumped resistance inserted at the connection point between the channel and the strike object. In analyzing lightning strikes to a grounded object using this channel representation, it is desirable to insert a several-hundred-ohm lumped resistor between the lightning channel and the strike object for simulating more realistic current reflection coefficient at the top of the strike object.

4. Excitations Used in Electromagnetic Return-Stroke Models

[46] In this section, we describe methods of excitation used to date in electromagnetic return-stroke models, and compare distributions of current along a vertical perfectly conducting wire above perfectly conducting ground corresponding to different excitation methods. Methods of excitation used in electromagnetic models are the following: (1) closing a charged vertical wire at its bottom end with a specified impedance (or circuit), (2) a delta-gap electric field source (same as voltage source), and (3) a lumped current source.

[47] Table 5 gives a list of papers on electromagnetic models of the lightning return stroke that are grouped into three categories depending on the method of excitation.

4.1. Closing a Charged Vertical Wire at Its Bottom End With a Specified Circuit

[48] *Podgorski and Landt* [1987] and *Podgorski* [1991] have represented a leader/return-stroke sequence by a precharged vertical resistive wire representing the lightning channel connected to the top of a vertical perfectly conducting wire representing the 553-m-high CN Tower via a nonlinear resistor. In their model, closing a charged vertical wire in a specified circuit constitutes excitation of the lightning return-stroke channel.

4.2. Delta-Gap Electric Field Source

[49] A delta-gap electric field source is located at ground surface [e.g., *Moini et al.*, 1998] or at the top of a grounded strike object [e.g., *Chai et al.*, 1994]. This type of source generates a specified electric field, which is independent of magnetic field surrounding the source or current flowing through it. This shows that a delta-gap electric field source has zero internal impedance. Hence its presence in series with the lightning channel and a strike object does not disturb any transient processes in them. If necessary, one could insert a lumped resistor in series with the delta-gap electric field source to adjust the impedance seen by waves entering the channel from the strike object to a value consistent with the expected equivalent impedance of the lightning channel.

4.3. Lumped Current Source

[50] A lumped current source is located at ground surface [e.g., *Grcev et al.*, 2003] or at the top of a grounded strike object [e.g., *Noda et al.*, 2005]. If reflected waves returning to the current source are negligible, the use of a lumped current source inserted at the attachment point does not cause any problem. This is the case for a branchless subsequent lightning stroke terminating on flat ground, in which upward connecting leaders are usually neglected and the return-stroke current wave propagates upward from the ground surface. The primary reason for the use of a lumped current source at the channel base is a desire to use directly the channel-base current, known from measurements for both natural and triggered lightning, as an input parameter of the model. When one employs a lumped ideal current source at the attachment point in analyzing lightning strikes to a tall grounded object, the lightning channel, owing to the infinitely large impedance of the ideal current source, is electrically isolated from the strike object, so that current waves reflected from ground cannot be directly transmitted to the lightning channel. Since this is physically unreasonable, a series ideal current source is not suitable for modeling of lightning strikes to tall grounded objects [*Baba and Rakov*, 2005a].

4.4. Comparison of Current Distributions Along a Vertical Perfectly Conducting Wire Excited by Different Sources

[51] In this section, we compare distributions of current along a vertical perfectly conducting wire in air energized by different methods of excitation described above. Figure 8 shows three such methods: closing a precharged vertical

Table 5. List of Papers on Electromagnetic Models of the Lightning Return Stroke Grouped Into Three Categories Depending on the Method of Excitation Employed

Excitation	Reviewed Journal Papers	Other Publications
Closing charged channel with a specified impedance	*Podgorski and Landt* [1987]	*Podgorski* [1991]
Delta-gap electric field source	*Moini et al.* [1998, 2000], *Baba and Ishii* [2001, 2003], *Kordi et al.* [2002, 2003b], *Mozumi et al.* [2003], *Pokharel et al.* [2003, 2004]	*Chai et al.* [1994], *Moini et al.* [1997], *Kato et al.* [1999, 2001], *Kordi et al.* [2003a], *Aniserowicz* [2004], *Miyazaki and Ishii* [2004, 2005], *Petrache et al.* [2005], *Bonyadi-ram et al.* [2005]
Lumped current source	*Baba and Rakov* [2003, 2005b], *Shoory et al.* [2005]	*Grcev et al.* [2003], *Maslowski* [2004], *Bonyadi-ram et al.* [2004], *Tatematsu et al.* [2004], *Noda et al.* [2005]

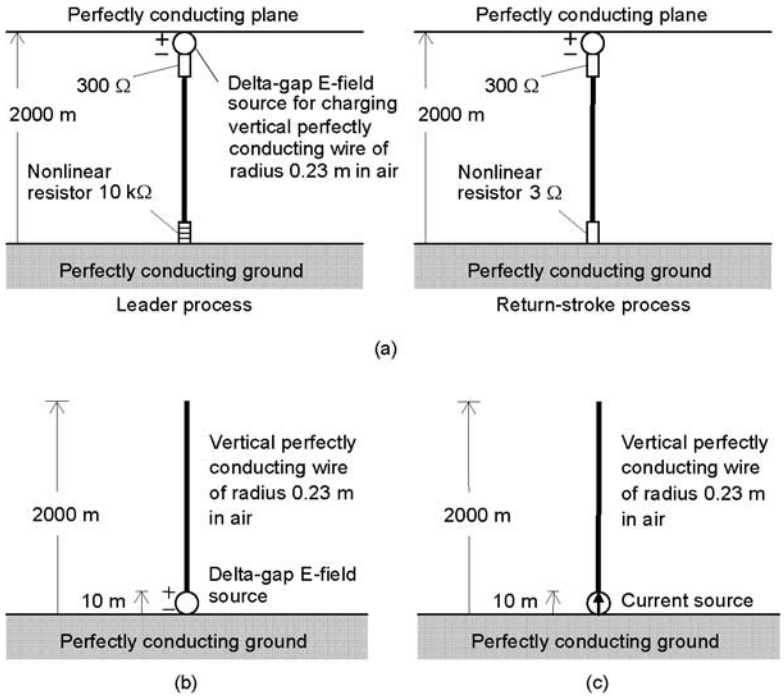

Figure 8. Three methods of excitation of the lightning channel above flat perfectly conducting ground: (a) a vertical perfectly conducting wire of radius 0.23 m in air that (left) is open-circuited at its bottom end when being charged by a delta-gap electric field source at its top and then (right) that connected to flat ground during its discharging, (b) a vertical perfectly conducting wire of radius 0.23 m in air excited at its bottom by a 10-m-long delta-gap electric field source, and (c) a vertical perfectly conducting wire of radius 0.23 m in air excited at its bottom by a 10-m-long lumped current source.

perfectly conducting wire of radius 0.23 m in air with a nonlinear resistor (Figure 8a) (left plot may be viewed as representing leader process and right plot the return-stroke process), a vertical perfectly conducting wire of radius 0.23 m in air excited at its bottom by a 10-m-long delta-gap electric field source (Figure 8b), and a vertical perfectly conducting wire of radius 0.23 m in air excited at its bottom by a 10-m-long lumped current source (Figure 8c). The delta-gap electric field source in the configuration shown in Figure 8a generates a ramp-front wave having a magnitude of 10 MV/m (100 MV along the 10-m-long source) and a risetime of 1 μs, while that shown in Figure 8b generates a ramp-front wave having a magnitude of 500 kV/m (5 MV along the 10-m-long source) and a risetime of 1 μs. The waveform of current injected by the lumped current source shown in Figure 8c is set to be the same as the waveform of current calculated for the bottom delta-gap electric field source shown in Figure 8b.

[52] Figure 9 shows distributions of current along the 0.23-m-radius vertical perfectly conducting wire in air excited by different sources (see Figure 8) that are calculated using the FDTD method. It is clear from Figures 9b and 9c that the distributions of current along the vertical wire excited at its bottom by the delta-gap electric field source and by the lumped current source are identical. Therefore resultant electric and magnetic fields generated around the vertical wire are also identical (the use of either delta-gap electric field or current source makes no difference in electric and magnetic fields in the case of lightning strike to flat ground if there are no downward reflections in the channel). It is clear from Figures 9a and 9b that the distribution of current along the charged vertical wire closed with the nonlinear resistor is similar to that along the same vertical wire excited at its bottom by the delta-gap electric field source.

5. Numerical Procedures Used in Electromagnetic Models of the Lightning Return Stroke

[53] In this section, we briefly describe numerical procedures used in electromagnetic models of the lightning return stroke, which include the following (in chronological order of their usage in electromagnetic models): (1) the MoM in the time domain, (2) the MoM in the frequency domain, and (3) the FDTD method.

[54] Table 6 includes a list of papers on electromagnetic models of the lightning return stroke grouped depending on the numerical procedure used.

5.1. Methods of Moments (MoMs) in the Time and Frequency Domains

5.1.1. MoM in the Time Domain

[55] The MoM in the time domain [*Van Baricum and Miller*, 1972; *Miller et al.*, 1973] is widely used in analyzing responses of thin-wire metallic structures to external time-varying electromagnetic fields. The entire conducting structure representing the lightning channel is modeled by a combination of cylindrical wire segments whose radii are

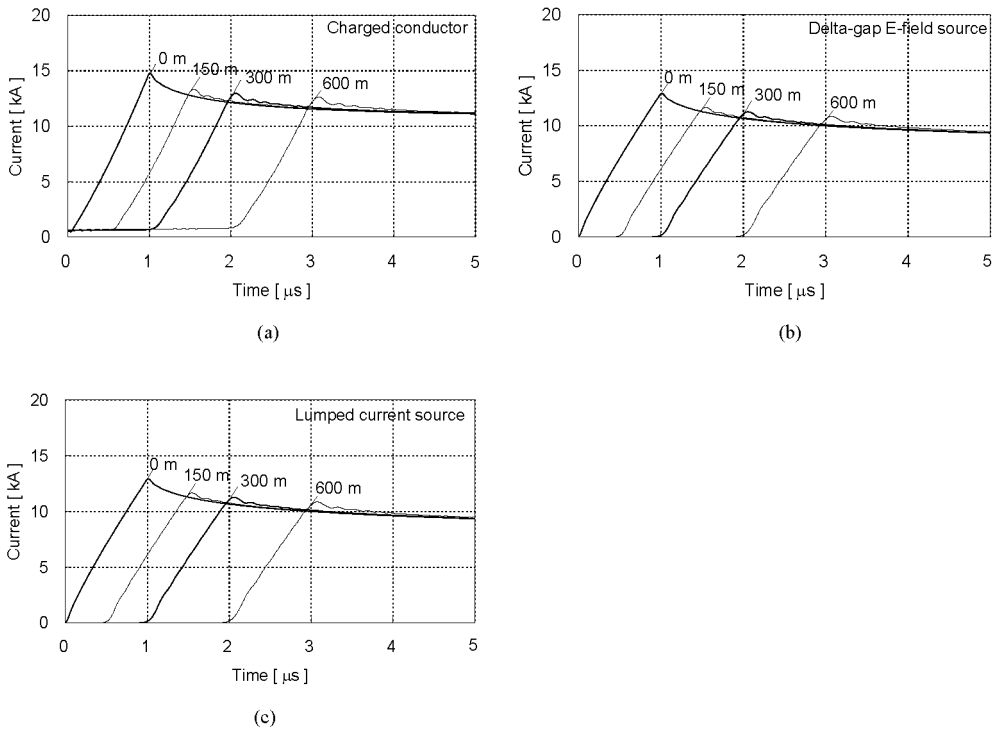

Figure 9. (a–c) Current waveforms at different heights along the lightning return stroke channel calculated using the FDTD method for three methods of excitation shown in Figures 8a–8c.

much smaller than the wavelengths of interest. Through numerically solving a so-called electric field integral equation, the time-dependent current distribution along the wire structure (lightning channel), excited by a lumped source, is obtained.

[56] The thin-wire time domain (TWTD) code [*Van Baricum and Miller*, 1972] (available from the Lawrence Livermore National Laboratory) is based on the MoM in the time domain. One of the advantages of the use of the time domain MoM is that it can incorporate nonlinear effects such as the lightning attachment process [e.g., *Podgorski and Landt*, 1987], although it does not allow lossy ground and wires buried in lossy ground to be incorporated.

5.1.2. MoM in the Frequency Domain

[57] The MoM in the frequency domain [*Harrington*, 1968] is widely used in analyzing the electromagnetic scattering by antennas and other metallic structures. In order to obtain the time-varying responses, Fourier and inverse Fourier transforms are employed. Current distribution along the lightning channel can be obtained numerically solving an electric field integral equation.

[58] This method allows lossy ground and wires in lossy ground (for example, grounding system of a strike object) to be incorporated into the model [*Burke and Miller*, 1984]. The commercially available numerical electromagnetic codes (e.g., NEC-2 [*Burke and Poggio*, 1980] and NEC-4 [*Burke*, 1992]) are based on the MoM in the frequency domain.

5.2. Finite Difference Time Domain (FDTD) Method

[59] The FDTD method [*Yee*, 1966] employs a simple way to discretize Maxwell's equations in differential form. In the Cartesian coordinate system, it requires discretization of the entire space of interest into small cubic or rectangular-parallelepiped cells. Since the material constants of each cell can be specified individually, a complex inhomogeneous medium can be analyzed easily.

[60] In order to analyze fields in unbounded space, an absorbing boundary condition has to be set on each plane which limits the space to be analyzed, so as to avoid reflections there. The FDTD method allows one to incorporate wires buried in lossy ground, such as strike-object

Table 6. List of Papers on Electromagnetic Models of the Lightning Return Stroke Grouped Into Three Categories Depending on the Numerical Procedure Used

Numerical Technique	Reviewed Journal Papers	Other Publications
MoM in the time domain	*Podgorski and Landt* [1987], *Moini et al.* [1998, 2000], *Kordi et al.* [2002, 2003b], *Mozumi et al.* [2003]	*Podgorski* [1991], *Moini et al.* [1997], *Kato et al.* [1999], *Kordi et al.* [2003a], *Bonyadi-ram et al.* [2004, 2005]
MoM in the frequency domain	*Baba and Ishii* [2001, 2003], *Pokharel et al.* [2003, 2004], *Shoory et al.* [2005]	*Chai et al.* [1994], *Kato et al.* [2001], *Grcev et al.* [2003], *Aniserowicz* [2004], *Maslowski* [2004], *Miyazaki and Ishii* [2004, 2005], *Petrache et al.* [2005]
FDTD method	*Baba and Rakov* [2003, 2005b]	*Tatematsu et al.* [2004], *Noda et al.* [2005]

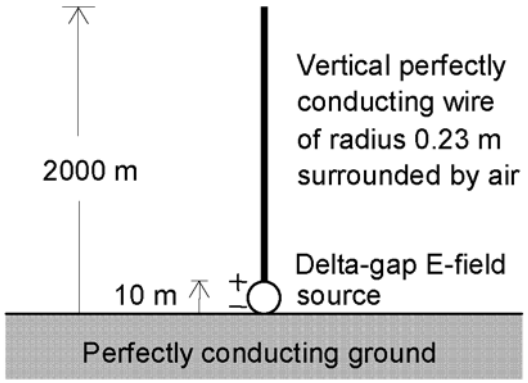

Figure 10. A vertical perfectly conducting wire of radius 0.23 m in air above perfectly conducting ground excited at its bottom by a 10-m-long delta-gap electric field source. The source produces a ramp-front wave having a magnitude of 500 kV/m (5 MV along the 10-m-long source) and a risetime of 1 μs. This configuration was used for comparison of different numerical procedures employed in electromagnetic models (see Figure 11).

grounding electrodes [*Noda et al.*, 2005], as well as nonlinear effects.

5.3. Comparison of Current Distributions Along a Vertical Perfectly Conducting Wire Calculated Using Different Numerical Procedures With Those Predicted by Chen's Analytical Equation

[61] In this section, we compare distributions of current along a channel-representing vertical wire, calculated using MoMs in the time and frequency domains and the FDTD method with that based on Chen's analytical equation (equation (1)) that is shown in Figure 1. Figure 10 shows configuration to be used for comparison of different numerical procedures: a vertical perfectly conducting wire of radius 0.23 m in air located above perfectly conducting ground and excited at its bottom by a 10-m-long delta-gap electric field source. The delta-gap electric field source produces a ramp-front wave having a magnitude of 500 kV/m (5 MV along the 10-m-long source) and a risetime of 1 μs. Figures 11a, 11b, and 11c show current waveforms at different heights calculated using the TWTD code (MoM in the time domain), the NEC-2 code (MoM in the frequency domain), and the FDTD method, respectively. As expected, waveforms calculated using the three different approaches agree well. Further, they all agree reasonably well with those calculated using Chen's analytical equation (see Figure 1).

[62] Note that, for the TWTD calculation, the 2000-m-long vertical wire was divided into 10-m-long segments and the response was calculated up to 5 μs with a 33.3-ns increment. For the NEC-2 calculation, the vertical wire was divided into 10-m-long segments, and the responses were calculated from 9.77 kHz to 10 MHz with a 9.77-kHz increment (corresponded to a time range from 0 to 102 μs with a 50-ns increment). In order to suppress nonphysical oscillations caused by the NEC-2, the vertical wire above 1500 m from the bottom was loaded by distributed series resistance. This resistive loading did not influence the response at the bottom ($z' = 0$) for the first 10 μs and that at a height of 600 m for the first 8 μs. For the FDTD calculation, the vertical wire of 0.23 m radius was replaced by a zero-radius perfectly conducting wire placed in the working volume of $60 \times 60 \times 2300$ m^3, which was divided into $1 \times 1 \times 10$ m^3 cells. When cells having a cross-sectional area of 1 m $\times$ 1 m are used and no modification is made for

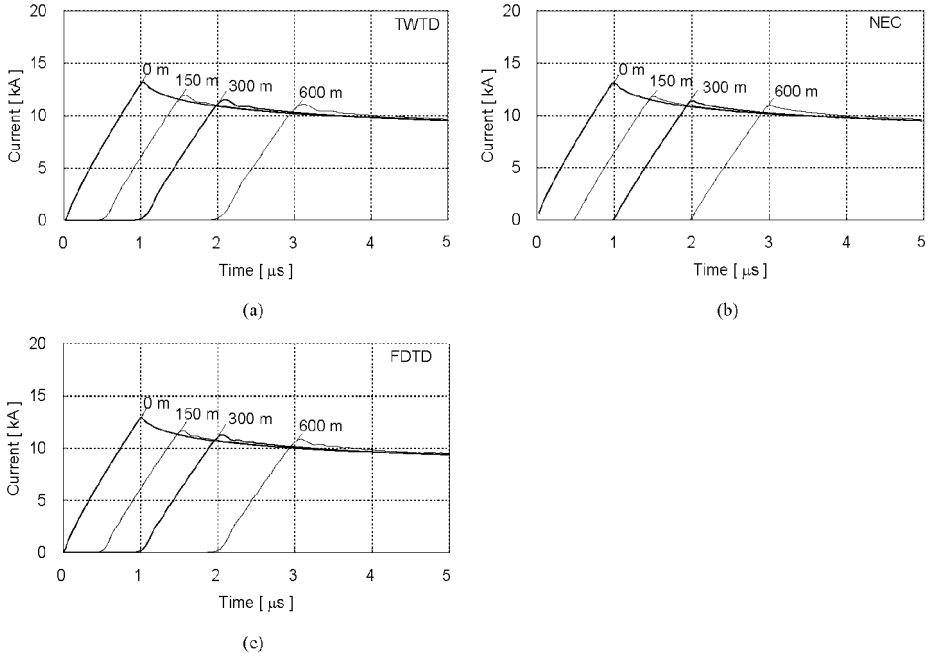

Figure 11. Current waveforms at different heights calculated using (a) the TWTD code (based on the MoM in the time domain), (b) the NEC-2 code (based on the MoM in the frequency domain), and (c) the FDTD method for the configuration shown in Figure 10.

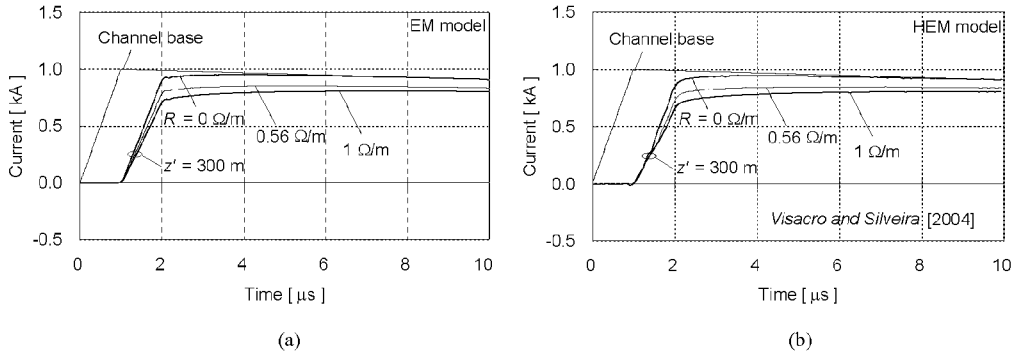

Figure A1. (a) Current waveforms at heights of 0 and 300 m along a 10-mm-radius vertical perfectly conducting or resistive wire, excited at its bottom by a lumped current source, calculated using an electromagnetic (EM) model based on the FDTD method, and (b) those calculated using the HEM model of *Visacro and Silveira* [2004].

relative permittivity and permeability of medium surrounding the wire, the vertical (z-directed) zero-radius perfectly conducting wire in air has an equivalent radius of 0.23 m [*Noda and Yokoyama*, 2002]. Perfectly matched layers (PML) [*Berenger*, 1994] (absorbing boundaries) were set at the top and sides of the working volume in order to avoid reflections there. The time increment was set to 2 ns.

6. Summary

[63] We have classified electromagnetic return-stroke models into four types depending on channel representation used to find the distribution of current along the channel: a perfectly conducting or resistive wire in air, a wire surrounded by dielectric (other than air), a wire loaded by additional distributed series inductance in air, and two wires having additional distributed shunt capacitance in air. It is desirable that models are capable of reproducing the following two features of the lightning return stroke: typical values of optically measured return-stroke wavefront speed ranging from $0.33c$ to $0.67c$, and the expected equivalent impedance of the lightning return-stroke channel in the range from 0.6 to 2.5 kΩ. As a current wave propagates upward along a vertical wire excited at its bottom by a lumped source, it necessarily suffers attenuation even if the wire has no ohmic losses. Mechanism of this attenuation is related to the boundary condition for the tangential electric field on the surface of the wire. The speed of current waves propagating along a vertical perfectly conducting wire in air above ground is essentially equal to the speed of light c, which is larger than typical values of measured return-stroke wavefront speed. The characteristic impedance of the wire ranges from 0.4 to 0.7 kΩ, which is somewhat lower than the expected equivalent impedance of the lightning return-stroke channel. When a vertical wire has distributed series resistance higher than 1 to 2 Ω/m, the apparent speed of current waves decreases appreciably with increasing the value of distributed resistance. The speed of current waves propagating along a vertical perfectly conducting wire surrounded by dielectric of relative permittivity ε_r ranges from $0.67c$ to $0.33c$ when ε_r ranges from 2.25 to 9. The corresponding characteristic impedance ranges from 0.13 to 0.47 kΩ, which is lower than the expected equivalent impedance of the lightning return-stroke channel. The speed of current waves propagating along a vertical perfectly conducting wire loaded by additional distributed series inductance L ranges from $0.67c$ to $0.33c$ when L ranges from 2.6 to 17 μH/m. The corresponding characteristic impedance ranges from 0.6 to 2.1 kΩ, which is similar to the expected equivalent impedance of the lightning return-stroke channel.

[64] Further, we have compared different methods of excitation used to date in electromagnetic return-stroke models: closing a charged vertical wire at its bottom with a specified impedance, a delta-gap electric field source, and a lumped current source. Distributions of current along the vertical perfectly conducting wire in air excited at its bottom by the delta-gap electric field source and by the lumped current source are identical. Also, the distribution of current along the charged vertical perfectly conducting wire closed with the nonlinear resistor is similar to that along the same wire excited at its bottom by the delta-gap electric field source.

[65] Also, we have compared distributions of current along a vertical perfectly conducting wire in air excited at its bottom by the delta-gap electric field source using different numerical procedures: MoMs in the time and frequency domains, and the FDTD method. As expected, distributions of current along the vertical perfectly conducting wire calculated using these three procedures agree well. They also agree reasonably well with those calculated using Chen's analytical equation.

[66] We have additionally found that the so-called hybrid electromagnetic (HEM) model predicts current distribution along the lightning channel that is consistent with that obtained using electromagnetic models.

Appendix A: Comparison of Current Distribution Along a Vertical Wire Calculated Using an Electromagnetic Model With That Predicted by the Hybrid Electromagnetic (HEM) Model

[67] The hybrid electromagnetic (HEM) model developed by *Visacro et al.* [2002] has been applied to modeling lightning return strokes [e.g., *Visacro and Silveira*, 2004]

and to analyzing the interaction of lightning with grounded objects [*Visacro and Soares*, 2005]. In the HEM model, electric and magnetic fields are decoupled (solution for electromagnetic fields is not a full-wave solution), but the electromagnetic field structure is not TEM. In the following, we compare the current distribution along a vertical wire excited at its bottom by a lumped current source above perfectly conducting ground calculated using the FDTD method with that predicted by the HEM model. The vertical wire has a radius of 10 mm and distributed series resistance of 0, 0.56, or 1 Ω/m. The 10-mm-radius wire is represented in the FDTD procedure by a zero-radius wire (simulated by forcing the longitudinal components of electric field along the axis of the wire to zero) embedded in cells for which the relative permittivity is set to an artificially lower value and the relative permeability to an artificially higher value [*Noda and Yokoyama*, 2002]. For our FDTD calculations we set ε_r and μ_r to 0.319 and 1/0.319, respectively. The current source generates a ramp wave having a magnitude of 1 kA, a risetime of 1 μs, and a decay time to the half-peak value of 50 μs. Figure A1 shows current waveforms at heights 0 and 300 m along the vertical wire calculated using the electromagnetic model based on the FDTD method and the HEM model. The HEM-calculated waveforms agree well with the FDTD-calculated waveforms.

[68] **Acknowledgments.** This research was supported in part by Doshisha University and by NSF grant ATM-0346164. The authors would like to acknowledge collaboration and useful discussions with (in alphabetical order) A. Ametani, K. Aniserowicz, S. Bonyadi-ram, V. Cooray, L. Grcev, A. M. Hussein, M. Ishii, W. Janischewskyj, S. Kato, B. Kordi, G. Maslowski, R. Moini, T. Mozumi, N. Nagaoka, R. K. Pokharel, F. Rachidi, G. Z. Rafi, M. Rubinstein, S. H. H. Sadeghi, V. O. Shostak, A. Shoory, F. Tesche, N. Theethayi, R. Thottappillil, M. A. Uman, and S. Visacro. The authors would also like to thank two anonymous reviewers for their helpful comments and suggestions.

References

Aniserowicz, K. (2004), A new algorithm for antenna theory modeling of a lightning return stroke, paper presented at 27th International Conference on Lightning Protection, Soc. de l'Electr., de l'Electron., et des Technol. de l'Inf. et de la Commun., Avignon, France.

Baba, Y., and M. Ishii (2001), Numerical electromagnetic field analysis of lightning current in tall structures, *IEEE Trans. Power Delivery*, *16*(2), 324–328.

Baba, Y., and M. Ishii (2003), Characteristics of electromagnetic return-stroke models, *IEEE Trans. Electromagn. Compat.*, *45*(1), 129–135.

Baba, Y., and V. A. Rakov (2003), On the transmission line model for lightning return stroke representation, *Geophys. Res. Lett.*, *30*(24), 2294, doi:10.1029/2003GL018407.

Baba, Y., and V. A. Rakov (2005a), On the use of lumped sources in lightning return stroke models, *J. Geophys. Res.*, *110*, D03101, doi:10.1029/2004JD005202.

Baba, Y., and V. A. Rakov (2005b), On the mechanism of attenuation of current waves propagating along a vertical perfectly conducting wire above ground: Application to lightning, *IEEE Trans. Electromagn. Compat.*, *47*(3), 521–532.

Baum, C. E., and L. Baker (1990) Analytic return-stroke transmission-line model, in *Lightning Electromagnetics*, pp. 17–40, Taylor and Francis, Philadelphia, Pa.

Berenger, J. P. (1994), A perfectly matched layer for the absorption of electromagnetic waves, *J. Comput. Phys.*, *114*, 185–200.

Bermudez, J. L., M. Rubinstein, F. Rachidi, F. Heidler, and M. Paolone (2003), Determination of reflection coefficients at the top and bottom of elevated strike objects struck by lightning, *J. Geophys. Res.*, *108*(D14), 4413, doi:10.1029/2002JD002973.

Bonyadi-ram, S., R. Moini, and S. H. H. Sadeghi (2004), Incorporation of distributed inductive loads in the antenna theory model of lightning return stroke channel, paper presented at 27th International Conference on Lightning Protection, Soc. de l'Electr., de l'Electron., et des Technol. de l'Inf. et de la Commun., Avignon, France.

Bonyadi-ram, S., R. Moini, S. H. H. Sadeghi, and V. A. Rakov (2005), Incorporation of distributed capacitive loads in the antenna theory model of lightning return stroke, paper presented at 16th International Zurich Symposium and Technical Exhibition on Electromagnetic Compatibility, Swiss Fed. Inst. of Technol., Zurich, Switzerland.

Burke, G. J. (1992), Numerical Electromagnetic Code (NEC-4)—Method of moments, *UCRL-MA-109338*, Lawrence Livermore Natl. Lab., Livermore, Calif.

Burke, G. J., and E. K. Miller (1984), Modeling antennas near to and penetrating a lossy interface, *IEEE Trans. Antennas Propag.*, *32*(10), 1040–1049.

Burke, G. J., and A. J. Poggio (1980), Numerical Electromagnetic Code (NEC)—Method of moments, *Tech. Doc. 116*, Nav. Ocean Syst. Cent., San Diego, Calif.

Chai, J. C., H. A. Heritage, and R. Briet (1994), Electromagnetic effects of the four-tower supported catenary wires array lightning protection system, paper presented at 16th International Aerospace and Ground Conference on Lightning and Static Electricity, Mannheim, Germany.

Chen, K. C. (1983), Transient response of an infinite cylindrical antenna, *IEEE Trans. Antennas Propag.*, *31*(1), 170–172.

Gomes, C., and V. Cooray (2000), Concepts of lightning return stroke models, *IEEE Trans. Electromagn. Compat.*, *42*(1), 82–96.

Gorin, B. N., and A. V. Shkilev (1984), Measurements of lightning currents at the Ostankino tower (in Russian), *Electrichestrvo*, *8*, 64–65.

Goubau, G. (1950), Surface waves and their application to transmission lines, *J. Appl. Phys.*, *21*, 1119–1128.

Grcev, L., F. Rachidi, and V. A. Rakov (2003), Comparison of electromagnetic models of lightning return strokes using current and voltage sources, paper presented at 12th International Conference on Atmospheric Electricity, Int. Comm. on Atmos. Electr., Versailles, France.

Harrington, R. F. (1968), *Field Computation by Moment Methods*, Macmillan, New York.

Inan, U. S., and N. G. Lehtinen (2005), Production of terrestrial gamma-ray flashes by an electromagnetic pulse from a lightning return stroke, *Geophys. Res. Lett.*, *32*, L19818, doi:10.1029/2005GL023702.

Kato, S., T. Narita, T. Yamada, and E. Zaima (1999), Simulation of electromagnetic field in lightning to tall tower, paper presented at 11th International Symposium on High Voltage Engineering, Inst. of Electr. Eng., London, U. K.

Kato, S., T. Takinami, T. Hirai, and S. Okabe (2001), A study of lightning channel model in numerical electromagnetic field computation (in Japanese), paper presented at 2001 IEEJ National Convention, Inst. of Electr. Eng. of Jpn., Nagoya, Japan.

Kordi, B., R. Moini, and V. A. Rakov (2002), Comment on "Return stroke transmission line model for stroke speed near and equal that of light" by R. Thottappillil, J. Schoene, and M. A. Uman, *Geophys. Res. Lett.*, *29*(10), 1369, doi:10.1029/2001GL014602.

Kordi, B., R. Moini, and V. A. Rakov (2003a), Comparison of lightning return stroke electric fields predicted by the transmission line and antenna theory models, paper presented at 15th International Zurich Symposium and Technical Exhibition on Electromagnetic Compatibility, Swiss Fed. Inst. of Technol., Zurich, Switzerland.

Kordi, B., R. Moini, W. Janischewskyj, A. M. Hussein, V. O. Shostak, and V. A. Rakov (2003b), Application of the antenna theory model to a tall tower struck by lightning, *J. Geophys. Res.*, *108*(D17), 4542, doi:10.1029/2003JD003398.

Krider, E. P. (1994), On the peak electromagnetic fields radiated by lightning return strokes toward the middle atmosphere, *J. Atmos. Electr.*, *14*, 17–24.

Lin, Y. T., M. A. Uman, J. A. Tiller, R. D. Brantley, W. H. Beasley, E. P. Krider, and C. D. Weidman (1979), Characterization of lightning return stroke electric and magnetic fields from simultaneous two-station measurements, *J. Geophys. Res.*, *84*(C10), 6307–6314.

Lu, G. (2006), Transient electric field at high altitudes due to lightning: Possible role of induction field in the formation of elves, *J. Geophys. Res.*, *111*, D02103, doi:10.1029/2005JD005781.

Maslowski, G. (2004), Some aspects of numerical modeling of lightning return stroke current based on antenna theory, paper presented at 27th International Conference on Lightning Protection, Soc. de l'Electr., de l'Electron., et des Technol. de l'Inf. et de la Commun., Avignon, France.

Mattos, M. A. da F., and C. Christopoulos (1988), A nonlinear transmission line model of the lightning return stroke, *IEEE Trans. Electromagn. Compat.*, *30*(3), 401–406.

Miller, E. K., A. J. Poggio, and G. J. Burke (1973), An integro-differential equation technique for the time-domain analysis of thin wire structures, *J. Comput. Phys.*, *12*, 24–48.

Miyazaki, S., and M. Ishii (2004), Influence of elevated stricken object on lightning return-stroke current and associated fields, paper presented at 27th International Conference on Lightning Protection, Soc. de l'Electr., de l'Electron., et des Technol. de l'Inf. et de la Commun., Avignon, France.

Miyazaki, S., and M. Ishii (2005), Lightning current distribution inside of directly hit building, paper presented at 14th International Symposium on High Voltage Engineering, IEEE Dielectr. and Electr. Insulation Soc., Beijing, China.

Moini, R., V. A. Rakov, M. A. Uman, and B. Kordi (1997), An antenna theory model for the lightning return stroke, paper presented at 12th International Zurich Symposium and Technical Exhibition on Electromagnetic Compatibility, Swiss Fed. Inst. of Technol., Zurich, Switzerland.

Moini, R., B. Kordi, and M. Abedi (1998), Evaluation of LEMP effects on complex wire structures located above a perfectly conducting ground using electric field integral equation in time domain, *IEEE Trans. Electromagn. Compat.*, *40*(2), 154–162.

Moini, R., B. Kordi, G. Z. Rafi, and V. A. Rakov (2000), A new lightning return stroke model based on antenna theory, *J. Geophys. Res.*, *105*(D24), 29,693–29,702.

Mozumi, T., Y. Baba, M. Ishii, N. Nagaoka, and A. Ametani (2003), Numerical electromagnetic field analysis of archorn voltages during a back-flashover on a 500 kV twin-circuit line, *IEEE Trans. Power Delivery*, *18*(1), 207–213.

Noda, T., and S. Yokoyama (2002), Thin wire representation in finite difference time domain surge simulation, *IEEE Trans. Power Delivery*, *17*(3), 840–847.

Noda, T., A. Tetematsu, and S. Yokoyama (2005), Improvements of an FDTD-based surge simulation code and its application to the lightning overvoltage calculation of a transmission tower, paper presented at International Conference on Power System Transients, Hydro-Quebec TransEnergie, Montreal, Que., Canada.

Nucci, C. A., G. Diendorfer, M. A. Uman, F. Rachidi, M. Ianoz, and C. Mazzetti (1990), Lightning return stroke current models with specified channel-base current: A review and comparison, *J. Geophys. Res.*, *95*(D12), 20,395–20,408.

Petrache, E., F. Rachidi, D. Pavanello, W. Janischewskyj, A. M. Hussein, M. Rubinstein, V. Shostak, W. A. Chisholm, and J. S. Chang (2005), Lightning strikes to elevated structures: influence of grounding conditions on currents and electromagnetic fields, paper presented at 2005 IEEE International Symposium on Electromagnetic Compatibility, Inst. of Electr. and Electron. Eng., Chicago, Ill.

Podgorski, A. S. (1991), Three-dimensional time domain model of lightning including corona effects, paper presented at 1991 International Aerospace and Ground Conference on Lightning and Static Electricity, NASA, Cocoa Beach, Fla.

Podgorski, A. S., and J. A. Landt (1987), Three dimensional time domain modelling of lightning, *IEEE Trans. Power Delivery*, *2*(3), 931–938.

Pokharel, R. K., M. Ishii, and Y. Baba (2003), Numerical electromagnetic analysis of lightning-induced voltage over ground of finite conductivity, *IEEE Trans. Electromagn. Compat.*, *45*(4), 651–666.

Pokharel, R. K., Y. Baba, and M. Ishii (2004), Numerical electromagnetic field analysis of transient induced voltages associated with lightning to a tall structure, *J. Electrostat.*, *60*(2), 141–147.

Rachidi, F., V. A. Rakov, C. A. Nucci, and J. L. Bermudez (2002), Effect of vertically extended strike object on the distribution of current along the lightning channel, *J. Geophys. Res.*, *107*(D23), 4699, doi:10.1029/2002JD002119.

Rakov, V. A. (1998), Some inferences on the propagation mechanisms of dart leaders and return strokes, *J. Geophys. Res.*, *103*(D2), 1879–1887.

Rakov, V. A. (2004), Lightning return stroke speed: a review of experimental data, paper presented at 27th International Conference on Lightning Protection, Soc. de l'Electr., de l'Electron., et des Technol. de l'Inf. et de la Commun., Avignon, France.

Rakov, V. A., and A. A. Dulzon (1987), Calculated electromagnetic fields of lightning return stroke (in Russian), *Tekh. Electrodin.*, *1*, 87–89.

Rakov, V. A., and W. G. Tuni (2003), Lightning electric field intensity at high altitudes: Inferences for production of elves, *J. Geophys. Res.*, *108*(D20), 4639, doi:10.1029/2003JD003618.

Rakov, V. A., and M. A. Uman (1998), Review and evaluation of lightning return stroke models including some aspects of their application, *IEEE Trans. Electromagn. Compat.*, *40*(4), 403–426.

Sadiku, M. N. O. (1994), *Elements of Electromagnetics*, Sounders Coll., Orlando, Fla.

Shoory, A., R. Moini, S. H. H. Sadeghi, and V. A. Rakov (2005), Analysis of lightning-radiated electromagnetic fields in the vicinity of lossy ground, *IEEE Trans. Electromagn. Compat.*, *47*(1), 131–145.

Tatematsu, A., T. Noda, and S. Yokoyama (2004), Simulation of lightning-induced voltages on a distribution line using the FDTD method, paper presented at International Workshop on High Voltage Engineering, Inst. of Electr. Eng. of Jpn., Sapporo, Japan.

Thottappillil, R., and M. A. Uman (1993), Comparison of lightning return-stroke models, *J. Geophys. Res.*, *98*, 22,903–22,914.

Thottappillil, R., V. A. Rakov, and M. A. Uman (1997), Distribution of charge along the lightning channel: Relation to remote electric and magnetic fields and to return-stroke models, *J. Geophys. Res.*, *102*, 6987–7006.

Thottappillil, R., J. Schoene, and M. A. Uman (2001), Return stroke transmission line model for stroke speed near and equal that of light, *Geophys. Res. Lett.*, *28*(18), 3593–3596.

Uman, M. A., D. K. McLain, and E. P. Krider (1975), The electromagnetic radiation from a finite antenna, *Am. J. Phys.*, *43*, 33–38.

Van Baricum, M., and E. K. Miller (1972), TWTD—A computer program for time-domain analysis of thin-wire structures, *UCRL-51-277*, Lawrence Livermore Natl. Lab., Livermore, Calif.

Visacro, S., and F. H. Silveira (2004), Evaluation of current distribution along the lightning discharge channel by a hybrid electromagnetic model, *J. Electrostat.*, *60*(2), 111–120.

Visacro, S., and A. Soares Jr. (2005), HEM: A model for simulation of lightning-related engineering problems, *IEEE Trans. Power Delivery*, *20*(2), 1206–1208.

Visacro, S. F., A. Soares Jr., and M. A. O. Schroeder (2002), An interactive computational code for simulation of transient behavior of electric system components for lightning currents, paper presented at 26th International Conference on Lightning Protection, Pol. Comm. on Lightning Prot. Cracow, Poland.

Wu, T. T. (1961), Transient response of a dipole antenna, *J. Math. Phys.*, *2*, 892–894.

Yee, K. S. (1966), Numerical solution of initial boundary value problems involving Maxwell's equations in isotropic media, *IEEE Trans. Antennas Propagat.*, *14*(3), 302–307.

Y. Baba, Department of Electrical Engineering, Doshisha University, Kyoto 610–0321, Japan. (ybaba@mail.doshisha.ac.jp)

V. A. Rakov, Department of Electrical and Computer Engineering, University of Florida, Gainesville, FL 32611, USA. (rakov@ece.ufl.edu)